

Non-rigid Surface Registration Using Spherical Thin-Plate Splines

Guangyu Zou¹, Jing Hua¹, and Otto Muzik²

¹ Department of Computer Science, Wayne State University, USA

² PET Center, School of Medicine, Wayne State University, USA

Abstract. Accurate registration of cortical structures plays a fundamental role in statistical analysis of brain images across population. This paper presents a novel framework for the non-rigid intersubject brain surface registration, using conformal structure and spherical thin-plate splines. By resorting to the conformal structure, complete characteristics regarding the intrinsic cortical geometry can be retained as a mean curvature function and a conformal factor function defined on a canonical, spherical domain. In this transformed space, spherical thin-plate splines are firstly used to explicitly match a few prominent homologous landmarks, and in the meanwhile, interpolate a global deformation field. A post-optimization procedure is then employed to further refine the alignment of minor cortical features based on the geometric parameters preserved on the domain. Our experiments demonstrate that the proposed framework is highly competitive with others for brain surface registration and population-based statistical analysis. We have applied our method in the identification of cortical abnormalities in PET imaging of patients with neurological disorders and accurate results are obtained.

1 Introduction

In order to better characterize the symptoms of various neuro-diseases from large datasets, automatic population-based comparisons and statistical analyses of integrative brain imaging data at homologous cortical regions are highly desirable in noninvasive pathophysiologic studies and disease diagnoses [1]. As a recent comparative study pointed out, intensity-based approaches may not effectively address the huge variability of cortical patterns among individuals [2]. Surface-based methods, which explicitly capture the geometry of the cortical surface and directly drive registration by a set of geometric features, are generally thought to be more promising in bringing homologous brain areas into accurate registration. One reason leading to this consideration is that the folding patterns (gyri and sulci) are typically used to define anatomical structures and indicate the location of functional areas [3].

In essence, cortical surfaces can be regarded as 3D surfaces. In the context of cortical structural analysis, representations based on the Euclidean distance are problematic, as it is not consistent with the intrinsic geometry of a surface [3]. For this reason, we adopted the strategy to first parameterize brain surface on a

canonical spherical domain using conformal mapping [4]. After that, subsequent matching and averaging of cortical patterns can be performed in this canonical space with enhanced efficiency since all geometric characteristics of the cortex are retained in this space. The benefits of this framework are as follows: first, because surface registration is modeled as a smooth deformation on a sphere, many confounding factors originally existing in the Euclidean space are eliminated; second, this registration method is implicitly scale-invariant as shapes are normalized on the canonical domain via conformal mapping; third, by means of deforming shapes in a parametric space, a 3D shape registration is reduced into a 2D space, thus largely simplifying computational complexity.

Even so, one needs to note that conformal mapping itself can not wipe off the inherent variability of individual human brains. To account for this nonlinear variation, non-rigid registration techniques need be used to deform one surface onto another with consistent alignment of primary anatomies. Towards this end, the spherical thin-plate splines (STPS) is presented to provide a natural scheme for this purpose. Given a set of point constraints, a smooth deformation field can be efficiently estimated with C^∞ continuity everywhere except at the location of landmarks where the continuity is C^1 . Optimization techniques can then be further appended afterwards in this framework as a back-end refinement in order to compensate for the discrepancies between piecewise spline estimation and the actual confounding anatomical variance.

For the purpose of accurately aligning two brain surfaces, a novel framework is systematically introduced in this paper. We first propose to use the conformal structure on a spherical domain to completely represent the cortical surface for registration. Building on that, we systematically derive the analytical and numerical solutions regarding spherical thin-plate splines (STPS) deformation and compound optimization based on the conformal factor and mean curvature of brain surfaces, which naturally induces a non-rigid registration between two brain surfaces. The effectiveness and accuracy of this framework is validated in a real application that intends to automatically identify PET abnormalities of the human brain.

2 Conformal Brain Surface Model

Based on *Riemannian geometry*, conformal mapping provides a mathematically rigorous way to parameterize cortical surface on a unit sphere, of which many properties have been well studied and fully controlled. Let ϕ denote this conformal transformation and (u, v) denote the spherical coordinates, namely, the conformal parameter. The cortical surface can be represented as a vector-valued function $\mathbf{f} : S^2 \rightarrow \mathbf{R}^3$, $\mathbf{f}(u, v) = (f_1(u, v), f_2(u, v), f_3(u, v))$. Accordingly, the local isotropic stretching of ϕ (conformal factor $\lambda(u, v)$) and the mean curvature $H(u, v)$ of surface \mathbf{f} can be treated as functions defined on S^2 . Since $\lambda(u, v)$ and $H(u, v)$ can uniquely reconstruct surface \mathbf{f} except for a rigid rotation [4], the two functions are sufficient for representing arbitrary closed shapes of genus zero topology. We term this representation the *Conformal Brain Surface Model*

(CBSM). The orientational freedom of CBSM can be removed by SVD methods, based on the landmark correspondences representing homologous cortical features. The CBSM is illustrated in Figure 1.

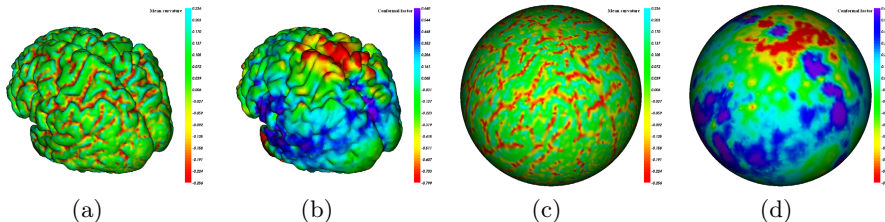


Fig. 1. Conformal Brain Surface Model. In (a) and (b), mean curvature and logarithmic conformal factor are color-encoded on the brain surface, respectively. (c) and (d) visualize the mean curvature function and the conformal factor function in accordance with the CBSM.

Suppose that M_1 and M_2 are two surfaces to be matched, and the parameterizations are $\varphi_1 : M_1 \rightarrow \mathbf{R}^2$ and $\varphi_2 : M_2 \rightarrow \mathbf{R}^2$, respectively. Then the transition map $\varphi_2 \circ \varphi_1^{-1} : M_1 \rightarrow M_2$ defines a bijection between M_1 and M_2 . Given a matching criterion, the registration of 3D shapes can be consequently defined as an automorphism μ on the parameter domain, such that the transformation $\psi = \varphi_2 \circ \mu \circ \varphi_1^{-1}$ in 3D minimizes the studied matching error. In particular, given a conformal parameterization of brain surface S , a registration criterion can be losslessly defined using $(\lambda(x_1, x_2), H(x_1, x_2))$.

A few related ideas have been proposed in [4,5,6,7,8]. However, Gu et al. [4] only pursued solutions in the conformal space, which in most cases is over-constrained for an optimal registration in terms of anatomy alignment. In [6], the deformation for the brain surface was essentially computed in a rectangular plane. Since a topological change is required from a sphere to a disk, choices for the landmarks are restricted by the large distortion at domain boundaries. The registration scheme employed in [7] is basically a variant of ICP (Iterated-Closest-Point) algorithm that is performed in the Euclidean space. As for the spherical deformation, diffeomorphic deformation maps constructed by the integration of velocity fields that minimize a quadratic smoothness energy under specified landmark constraints are presented in a recent paper [9]. When compared with STPS, its solution does not have closed-form.

3 Method

Generally, our method includes two main steps: First, the registration is initiated by a feature-based STPS warping. This explicit procedure largely circumvents local minimum and is more efficient when compared with using variational optimization directly. Second, a compound energy functional that represents a balanced measurement of shape matching and deformation regularity is minimized,

which compensates for the potential improper localization of unmarked cortical features.

3.1 STPS Deformation

Thin-plate splines (TPS) are a class of widely used non-rigid interpolating functions. Because of its efficiency and robustness, intensive exploitation of TPS has been made for smooth data interpolation and geometric deformation.

The spherical analogue of the well-known thin-plate bending energy defined in Euclidean space was formulated in [10], which has the form

$$J_2(u) = \int_0^{2\pi} \int_0^\pi (\Delta u(\theta, \phi))^2 \sin \phi d\theta d\phi, \quad (1)$$

where $\theta \in [0, \pi]$ is latitude, $\phi \in [0, 2\pi]$ is longitude, Δ is the Laplace-Beltrami operator. Let

$$K(X, Y) = \frac{1}{4\pi} \int_0^1 \log h \left(1 - \frac{1}{h}\right) \left(\frac{1}{\sqrt{1 - 2ha + h^2} - 1} - 1\right) dh, \quad (2)$$

where $a = \cos(\gamma(X, Y))$ and $\gamma(X, Y)$ is the angle between X and Y . With the interpolants

$$u(P_i) = z_i, \quad i = 1, 2, \dots, n, \quad (3)$$

the solution is given by

$$u_n(P) = \sum_{i=1}^n c_i K(P, P_i) + d, \quad (4)$$

where

$$\begin{aligned} \mathbf{c} &= \mathbf{K}_n^{-1} [\mathbf{I} - \mathbf{T}(\mathbf{T}^T \mathbf{K}_n^{-1} \mathbf{T})^{-1} \mathbf{T}^T (\mathbf{K}_n^{-1})] \mathbf{z}, \\ d &= (\mathbf{T}^T \mathbf{K}_n^{-1} \mathbf{T})^{-1} \mathbf{T}^T (\mathbf{K}_n^{-1}) \mathbf{z}, \\ (\mathbf{K}_n)_{ij} &= K(P_i, P_j), \\ \mathbf{T} &= (1, \dots, 1)^T, \\ \mathbf{z} &= (z_1, \dots, z_n)^T, \end{aligned}$$

in which \mathbf{K}_n is the $n \times n$ matrix with its (i, j) th entry denoted as $(\mathbf{K}_n)_{ij}$.

Given the displacements $(\Delta\theta_i, \Delta\phi_i)$ of a set of points $\{P_i\}$ on the sphere in spherical coordinates, the STPS can be used to interpolate a deformation map $S^2 \rightarrow S^2$ that is consistent with the assigned displacements at $\{P_i\}$ and smooth everywhere, which minimizes J_2 . Most anatomical features on brain surfaces, such as sulci and gyri, are most appropriate to be represented as geometric curves. The feature curves are automatically fitted using the cardinal splines, based on a set of sparse points selected by a neuroanatomist on the native brain surface. The framework also provides the automatic landmark tracking functions using the methods in [11]. In order to deal with curve landmarks on the

sphere with STPS, we convert a curve to a dense set of ordered points, yielding precise control over curves. A global smooth deformation field $(u_\theta(P), u_\phi(P))$ can be consequently determined, which warps each landmark curve on the source CBSM into their counterpart on the target as shown in Figure 2 (a), (b) and (c). This deformation ensures the alignment of primary labeled features. However, other unlabeled cortical anatomies are not guaranteed to be perfectly matched to their counterparts. In the following, a global optimization scheme is proposed to address this issue.

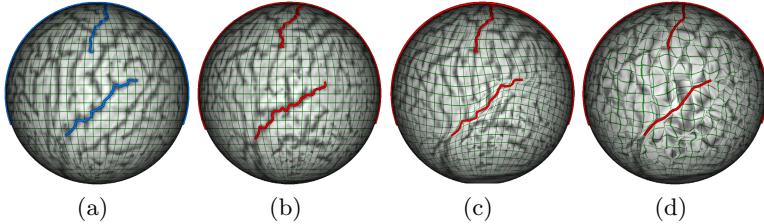


Fig. 2. The illustration of the CBSM deformations at each registration stage. (a) shows the target CBSM. (b) shows the source CBSM. (c) shows the effect of STPS deformation performed on (b). The result of a further refining optimization is shown in (d).

3.2 Compound Optimization

Since all the transformations applied so far are topology preserving, we generally consider that homologous anatomies have been laid very close to each other in the spherical space through the landmark-based STPS deformation. To further refine the alignment of anatomies besides the manually traced features, we define a global distance in the shape space via CBSM based on the conformal factor $\lambda(u, v)$ and the mean curvature $H(u, v)$:

$$d(S_1, S_2) = \int_{S^2} ((\log \lambda_1(u, v) - \log \lambda_2(u, v))^2 + (H_1(u, v) - H_2(u, v))^2) d\mu, \quad (5)$$

where the $d\mu$ is the area element of the unit sphere S^2 . Here we compare the logarithm values of λ to eliminate the bias between the same extent of stretching and shrinking from conformal mapping. When this functional is minimized, two brain surfaces are registered. Additionally, we moderately smooth down the brain surface for mean curvature computation similar in spirit to [3], since we assume that the optimization should only be directed by large-scale geometric features while being relatively insensitive to those small folds that are typically unstable across subjects. Suppose the optimization procedure is performed by deforming S_2 to S_1 . The optimal nonlinear transformation $\tilde{\phi}^*$ can be formulated as

$$\tilde{\phi}^* = \arg \min_{\phi} (d(S_1(u, v) - S_2(\phi(u, v)))). \quad (6)$$

In practice, simply minimizing the distance functional may cause undesirable folds or distortions in the local patch. To avoid this, we also add another term

to the distance functional to maximize conformality while warping two spherical images into registration. This regularizing term is essentially a harmonic energy functional.

Note that the cortical surface, as well as the domain, are approximated by triangular meshes. We use the gradient descent method for the numerical optimization. Suppose $\mathbf{f}(\cdot)$ and $\mathbf{g}(\cdot)$ are the piecewise linear approximations of CBSM domains, p and q are neighbor vertices, and $\{p, q\}$ denotes the edge spanned between them. $\alpha_{p,q}$ and $\beta_{p,q}$ denote the two angles opposite to p, q in the two triangles sharing edge $\{p, q\}$. $A_{f(g)}(p)$ denotes the areal patch in $f(g)$ associated with p . Therefore, the gradient of this compound functional is given by

$$\begin{aligned} \frac{\partial E}{\partial \mathbf{f}(v)} = & \sum_{u \in N_1(v)} (\cot \alpha_{p,q} + \cot \beta_{p,q})(\mathbf{f}(v) - \mathbf{f}(u)) \\ & + \frac{\varphi A_f(v)}{\sum_{i \in K_f} A_f(i)} \lambda_{f-g}(v) \nabla_{\overrightarrow{\{u^*, v\}}} \lambda_{f-g}(v) \\ & + \frac{\omega A_f(v)}{\sum_{i \in K_f} A_f(i)} H_{f-g}(v) \nabla_{\overrightarrow{\{u^*, v\}}} H_{f-g}(v), \end{aligned} \quad (7)$$

where φ and ω are tunable weighting factors, $SF_{f-g}(\cdot) = SF_f(\cdot) - SF_g(\cdot)$, and u^* is defined as

$$u^*(v) = \arg \max_{u \in N_1(v)} \nabla_{\overrightarrow{\{u, v\}}} (SF_f - SF_g)(v), \quad (8)$$

in which the SF denotes either $\lambda(\cdot)$ or $H(\cdot)$, and $N_1(v)$ is the 1-ring neighbors of v . In practice, we also constrain the displacement of each vertex in the tangential space of the unit sphere. The optimized result after STPS deformation is shown in Figure 2 (d). Its improvement to brain surface registration will be further demonstrated in Section 4.

4 Experiments

We have tested our framework through automatic identification of Positron Emission Tomography (PET) abnormalities. In order to identify the functional abnormalities characterized by PET, the normal fusion approach [12] is used for MRI and PET integration as shown in Figure 3 (a) and (b). PET values are projected onto the high resolution brain surface extracted from MRI data. Then we apply the proposed framework to bring the studied subjects (high-resolution cortical surfaces) into registration and subdivide the cortical surfaces into registered, homotopic elements on the spherical domain. Similar to the element-based analysis of PET images in [13,14], we obtain the PET concentration for each of the cortical elements. A patient's data is compared with a set of normals to locate the abnormal areas in the patient brain based on the statistical histogram analysis of the PET concentration at the homotopic cortical elements. Figure 3 (c)

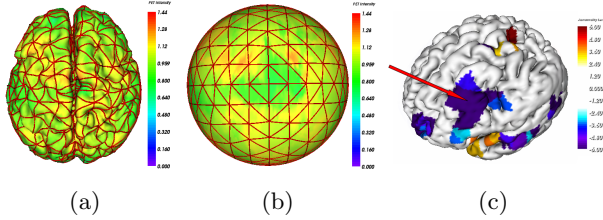


Fig. 3. Identification of PET abnormalities. (a) and (b) show the rendering of the PET concentration on the cortical surface and the spherical domain, respectively. The triangle-like elements are the defined homotopic cortical elements by the registration. (c) PET abnormalities are rendered on the cortical surface using a color map.

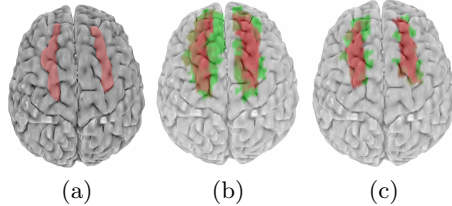


Fig. 4. Repetition Levels for Prominent Cortical Regions. (a) shows the regions of middle frontal gyri delineated by a neuroscientist; (b) shows the agreement using only STPS, while (c) gives the result when the compound optimization is enabled.

show the result of a pediatric patient with epilepsy. The blue color indicates decreased tracer concentration than normal. We use 8 normal pediatric datasets to establish the normal distribution for comparison. One of the normal dataset is treated as the template for registration. In our experiments, the detected abnormal spots well corresponds to the final clinical diagnoses because the high-quality inter-subject mapping and registration greatly improves cross-subject element matching for statistical analysis. This real application validates the registration capability of our framework from a practical perspective.

We also directly evaluated our methods on several prominent neuroanatomical regions in terms of group overlap using high-resolution MRI data. Since cortical regions have been well defined and indexed by elements, the overlap can be measured by area. The elements for a specific feature which agree on more than 85% cases are colored in red. Those that agree on 50%~85% cases are colored in green. As an example, Figure 4 demonstrates the result on middle frontal gyri, delineated by a neuroscientist. It is evident that, after compound optimization, the features under study appear more consistent to the middle frontal gyrus regions on the template cortex because of the refined matching of geometric structures by compound optimization. The certainty with regard to the regional boundaries are increased. More comprehensive experiments indicate that significant agreements can be achieved via our method. The overall registration accuracy in terms of group overlap is about 80%.

5 Conclusion

We have presented a novel, effective non-rigid brain surface registration framework based on conformal structure and spherical thin-plate splines. To enable this procedure, we systematically derive the analytical and numerical solutions regarding STPS deformation and compound optimization based on the conformal factor and mean curvature of brain surfaces. Our experiments demonstrate that our method achieves high accuracy in terms of homologous region overlap. Our method is tested in a number of real neurological disorder cases, which consistently and accurately identify the cortical abnormalities.

References

1. Thompson, P., et al.: Mapping cortical change in alzheimer's disease, brain development and schizophrenia. *NeuroImage* 23(1), S2–S18 (2004)
2. Hellier, P., et al.: Retrospective evaluation of intersubject brain registration. *IEEE TMI* 22(9), 1120–1130 (2003)
3. Fischl, B., et al.: Cortical surface-based analysis II: Inflation, flattening, and a surface-based coordinate system. *NeuroImage* 9(2), 195–207 (1999)
4. Gu, X., et al.: Genus zero surface conformal mapping and its application to brain surface mapping. *IEEE TMI* 23(8), 949–958 (2004)
5. Fischl, B., et al.: High-resolution intersubject averaging and a coordinate system for the cortical surface. *Human Brain Mapping* 8(4), 272–284 (1999)
6. Wang, Y., et al.: Optimization of brain conformal mapping with landmarks. In: Proc. MICCAI 2005, pp. 675–683 (2005)
7. Tosun, D., et al.: Mapping techniques for aligning sulci across multiple brains. *Medical Image Analysis* 8(3), 295–309 (2004)
8. Zou, G., et al.: An approach for intersubject analysis of 3D brain images based on conformal geometry. In: Proc. ICIP 2006 pp. 1193–1196 (2006)
9. Glaunès, J., et al.: Landmark matching via large deformation diffeomorphisms on the sphere. *Journal of Mathematical Imaging and Vision* 20, 179–200 (2004)
10. Wahba, G.: Spline interpolation and smoothing on the sphere. *SIAM Journal of Scientific and Statistical Computing* 2(1), 5–16 (1981)
11. Lui, L.M., et al.: Automatic landmark tracking and its application to the optimization of brain conformal mapping. In: Proc. CVPR 2006 pp. 1784–1792 (2006)
12. Stockhausen, H.V., et al.: 3D-tool - a software system for visualisation and analysis of coregistered multimodality volume datasets of individual subjects. *NeuroImage* 7(4), S799 (1998)
13. Ghias, S.A.: GETool: Software tool for geometric localization of cortical abnormalities in epileptic children. Master Thesis, Computer Science Department, Wayne State University (2006)
14. Muzik, O., et al.: Multimodality Data Integration in Epilepsy. *International Journal of Biomedical Imaging* 13963 (2007)